Sensor Network Localization by Augmented Dual Embedding

Shai Gepshtein and Yosi Keller

***Abstract*—In this work we propose an anchor-based sensor networks localization scheme that utilizes a dual spectral embedding. The input noisy distance measurements are first embedded by Diffusion embedding and then by Isomap. This allows to better estimate the intrinsic network geometry and derive improved adaptive bases, that are used to estimate the global localization via L_1 regression. We then introduce the Augmented Dual Embedding by computationally augmenting the set of measured distances and computing the dual embedding. This significantly improves the scheme's robustness and accuracy. We also propose a straightforward approach to preprocessing the noisy distances via the triangle inequality. The proposed scheme is experimentally shown to outperform contemporary state-of-the-art localization schemes.**

***Index Terms*— Graph theory, machine learning, network theory (graphs), wireless sensor networks.**

I. Introduction

THE effective use of sensor networks entails computational challenges. One of which is the sensor network localization (SNL) problem, where one aims to estimate the absolute positions of the sensors based on noisy, inaccurate and incomplete (sparse) inter-sensor distance measurements. This is depicted in Fig. 1, where a sensor network is placed over a set of US cities, and each sensor measures its distance to small subset of sensors in its spatial vicinity. These measurements are often noisy due to the use of RF technology for their estimation.

A sensor network comprises of sensors randomly dispensed at positions $S = \{\mathbf{x}_i\}_1^N$, where each sensor communicates with its neighboring nodes within a limited sensing range R_0, and is able to estimate their distance. The sensing range limitation R_0 is due to energetic constraints induced by the small size and price of each sensor, and this is commonly denoted as the *unit disc model*. The sensors' location can be accurately estimated by equipping each sensor with a GPS device. However, such an approach would make each sensor costlier, larger in size and significantly more energy consuming. Moreover, in some common settings such as indoor environments (museums, shopping malls, etc.), or due to particular line-of-sight conditions, some sensors might be unable to acquire the GPS signal.

Manuscript received May 06, 2014; revised November 22, 2014 and January 31, 2015; accepted February 05, 2015. Date of publication March 06, 2015; date of current version April 06, 2015. The associate editor coordinating the review of this manuscript and approving it for publication was Dr. Branko Ristic.

The authors are with the Faculty of Engineering, Bar Ilan University, Ramat Gan 52900, Israel (e-mail: shaigep@gmail.com; yosi.keller@gmail.com).

Color versions of one or more of the figures in this paper are available online at http://ieeexplore.ieee.org.

Digital Object Identifier 10.1109/TSP.2015.2411211

Thus, a common approach is to use a heterogenous set of sensors consisting of two classes. The first comprises of $K \ll N$ (typically $K = O(10^{-2}) \cdot N$) nodes equipped with a GPS device, able to independently and accurately estimate their position. These nodes are denoted as *anchors*, while the other nodes can only estimate inter-sensor distances within R_0.

The SNL problem is to localize the sensors S given the positions of the $K \ll N$ anchors, and a noisy estimate of a small subset (down to 5%) of the pairwise Euclidean distances $\mathbf{D} = \{d_{ij}\}$ between each sensor and some of its neighbors (Fig. 1). The common distance measurement model [1]–[7] is given by

$$d_{ij} = d_{ij}^0(1+f), f \sim N\left(0, \sigma_n^2\right), \tag{1}$$

where d_{ij}^0 is the true (unknown) distance

$$d_{ij}^0 = \|\mathbf{x}_i - \mathbf{x}_j\|_2, \tag{2}$$

and negative noisy distance values $d_{ij} < 0$ are truncated to zero. In some situations, in order to further decrease the energetic costs of communications and range estimation, only Q edges are retained at most per node, while others use the *unit disk model* [6] where the distances *to all* nodes within R_0 are used. Some works deal with the *anchor-free* formulation [2], [3], [6], where no anchor positions are given.

Let $\{\mathbf{x}_i\}_1^N$ be the set of estimated sensor positions. In the SNL problem we aim to recover $\{\mathbf{x}_i\}_1^N$, such that their distances adhere to the noisy measured distances. The localization can be formulated as an optimization problem

$$\{\mathbf{x}_i\}_1^N = \arg \min_{\{\mathbf{x}_i^*\}_1^n} \sum_{i,j \ s.t. \ d_{ij}>0} \left(\left\|\mathbf{x}_i^* - \mathbf{x}_j^*\right\|_2^2 - d_{ij}^2\right)^2. \tag{3}$$

As the objective function in (3) is nonconvex, Biswas *et al.* [1] applied SDP relaxation to

$$\{\mathbf{x}_i\}_1^N = \arg \min_{\{\mathbf{x}_i^*\}_1^n} \sum_{i,j \ s.t. \ d_{ij}>0} \left|\left\|\mathbf{x}_i^* - \mathbf{x}_j^*\right\|_2^2 - d_{ij}^2\right|. \tag{4}$$

Another variation of the objective function is given by

$$\{\mathbf{x}_i\}_1^n = \arg \min_{\{\mathbf{x}_i^*\}_1^n} \sum_{i,j \ s.t. \ d_{ij}>0} \left(\left\|\mathbf{x}_i^* - \mathbf{x}_j^*\right\|_2 - d_{ij}\right)^2 \tag{5}$$

and solved by the stress majorization algorithm (SMACOF) [8].

Other approaches [6], [9], [10] start by localizing small network patches, and synchronizing the set of patches by computing their relative reflection, rotation and translation. In this work we follow the school of thought proposed by Weinberger *et al.* [4] and later used by Keller *et al.* [7]. In these works the

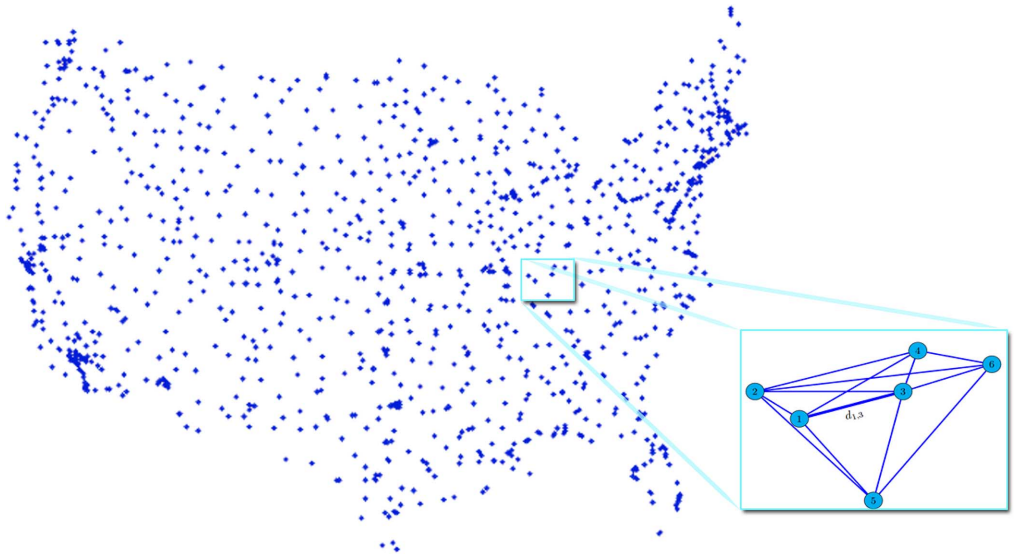

Fig. 1. The sensor localization problem. The sensor network consists of a set of sensor positioned in US cities. Each sensor can measure its distance to a small subset of sensors in its geographical vicinity.

localization is formulated in an embedding domain, that utilizes the low dimensional intrinsic geometrical structure of the network.

Although these approaches proved efficient, some aspects were overlooked by Keller *et al.* [7], and are at the heart of the proposed work. First, they formulated the localization as a regression problem over a general graph, without explicitly utilizing the (*a priori* known) intrinsic planarity (two-dimensional flatness) of the estimated manifold and graph. Second, in that work the graph was constructed using the given noisy sensor-to-sensor distances, while patch based SNL schemes [6], [9], [10] demonstrated that sensor patches can be accurately localized. Hence, sensor patches can be used to robustly estimate sensor-to-sensor distances, based on the distances of the *multiple* sensors comprising each sensor patch. In particular, the distance measurements' noise is assumed to be independent across different distance measurements, implying that sensor-to-sensor distance estimates can be improved utilizing multiple noisy sensor-to-sensor measurements. Last, the SNL problem is related to geometrical constraints, such as the triangle inequality. By deriving a computational approach that implements these extensions to our previous work [7], the SNL accuracy can be improved, as depicted in Fig. 2.

Following these themes, we aim to study the anchor-based SNL problem, and propose the following contributions:

First, we study the properties of the adaptive Diffusion regression bases introduced by Keller *et al.* [7], and note that due to the noisy distance measurements they often provide a high dimensional embedding rather than a two-dimensional one, as expected for two-dimensional planar networks. To resolve that we derive the Dual Embedding Spectral Regression (DESR) scheme, where the Diffusion bases are further embedded using Isomap [11], and the resulting dual embedding basis functions are used for regression. This is exemplified in Fig. 3.

Second, We computationally augment the set of distance measurements using patch-based localization schemes [6], [9], [10], where the nodes are first clustered and localized in small patches. The resulting network is denser and the inter-patch distances are more accurate as neighboring patches are connected by multiple edges. We apply the DESR localization to the augmented network and show that this improves the localization robustness, and reduces its failures due to localization foldovers.

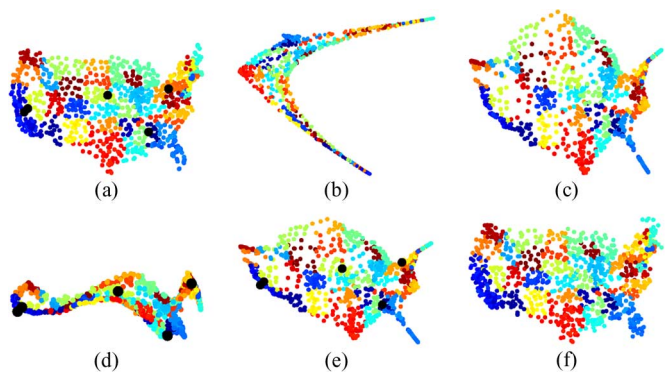

Fig. 2. The proposed sensors localization scheme. (a) Groundtruth true positions and anchor points. (b) The two leading Diffusion embedding eigenfunctions (basis functions). (c) The two leading Dual embedding basis functions. (d) and (e) show the spectral regression localization of the input five anchor points for (b) and (c), respectively (f) ADESR localization results.

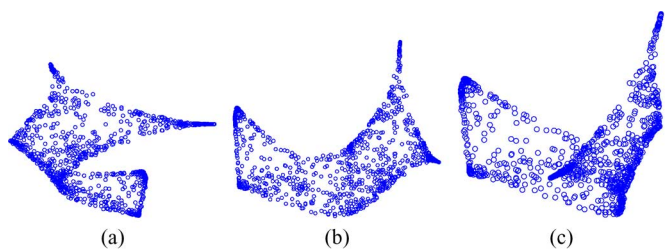

Fig. 3. The three leading embedding vectors of the Diffusion embedding shown from different viewing angles. They constitute a plane embedded in a three-dimensional space.

Last, we propose to explicitly integrate geometrical constraints into our scheme by inducing the triangle inequality by preprocessing the augmented sensor network and show that this further improves the localization accuracy.

The paper is organized as follows: we review contemporary SNL approaches in Section II, and recall the Diffusion approach to SNL in Section III. The proposed DESR and ADESR schemes are introduced in Section IV, and experimentally verified and compared to contemporary state-of-the-art approaches in Section V. Concluding remarks and future extensions are discussed in Section VI.

II. Background

The sensor network localization (SNL) problem has attracted a significant research effort. The first class of approaches aimed to minimize the straightforward localization formulations as in (3)–(5) that can be relaxed into a convex SDP problems [12]–[15] or second order cone (SOCP) problem [16], [17] by transforming the quadratic constraints into inequalities. For noiseless systems the SDP algorithm is guaranteed to estimate the unique solution in polynomial time [14]. However, this approach leads to high dimensional solutions that are projected to the plane and might result in significant estimation errors. Moreover, SDP based methods might be unfeasible for large networks as they become too exhaustive to compute.

Graph rigidity was studied by Eren *et al.* [18] as a mean of analyzing the feasibility of localizing sensor networks given noisy and partial distance measurements. The lack of graph rigidity is often manifested by localization foldovers, leading to significant localization errors.

A different class of schemes starts by first localizing small rigid sensors patches and then stitching them together to recover the global configuration. For instance, the patch embedding scheme proposed by Moore *et al.* [19], localized four nodes in regions constructed from robust quadrilaterals forming a complete graph whose relative positions are robust to measurement noise. Neighboring quadrilaterals are iteratively merged, and the result is improved by stress minimization. Koren *et al.* [9] proposed the PATCHWORK global localization approach consisting of two stages. First, patches are localized by estimating missing distances by averaging lower and upper bounds based on the triangle inequality. The full graph of each patch is then localized using MDS, and the result is refined by stress majorization. The localized rigid patches are mapped to a global coordinate system using affine transformation estimated by using their common overlaps.

The As-Rigid-As-Possible (ARAP) and As-Affine-As-Possible (AAAP) approaches, introduced by Zhang *et al.* [10], follow a similar path. The ARAP starts by localizing rigid patches, and estimating their relative rigid transformations. The global coordinate are recovered by solving a set of nonlinear equations. In the AAAP scheme, the relative transformation is estimated by an affine transformation. Cucuringu *et al.* [6] proposed the As-Synchronized-As-Possible (ASAP) scheme, which is an anchor-free scheme that can incorporate the positions of anchors. The ASAP starts by localizing small network patches, and the global synchronization is computed by sequentially estimating the reflections and the rotations using a spectral synchronization scheme, and the translations by solving a set of linear equations.

TABLE I
Sensor Networks Localization Schemes. "Strictly Anchor-Based" Schemes Have to Use Anchors, While "Potentially Anchor-Based" Schemes can Incorporate Anchors Information, but can be Applied Without It. "SDP" Schemes Utilize SDP-Based Optimization. A '+' Sign Implies That a Scheme has a Particular Property (Such as "Strictly Anchor-Based" etc), While a '−' Sign Implies That it Does Not

	Strictly anchor-based	**Potentially anchor-based**	**SDP**
PATCHWORK [10]	-	-	-
MVU [21]	-	+	+
ARAP [11]	-	+	-
DESR [8]	+	+	-
ASAP [7]	-	+	-

Dimensionality reduction and embedding schemes were also applied to sensor localization. Weinberger *et al.* [20] proposed an Maximum Variance Unfolding (MVU) embedding that provides a low-dimensional representation of the coordinates, yielding a low dimensional SDP problem that is solved via quadratic programming. The result is further refined by applying conjugate gradient descent to (3). The Locally-Rigid Embedding was introduced by Singer [21] to recover the global configuration, by computing spatial local weights in the vicinity of each sensor. These weights were agglomerated via a spectral decomposition to yield the global solution.

An anchor-based SNL scheme based on the Diffusion framework was introduced by Keller *et al.* [7], that derived data adaptive bases and frames, by computing the Graph Laplacian of the sensor network. By choosing a suitable kernel, the Laplacian computed using the sparse set of inter-sensor distances, approximates the Laplacian of the full network. The X and Y coordinates are extrapolated using the adaptive bases. A multiresolution diffusion scheme is derived using a Diffusion frame consisting of a set of bases related to a corresponding set of kernel bandwidths, where the estimation is conducted using L_1 regression.

Dual embedding in the Diffusion domain was proposed by Meyer *et al.* [22] for the unsupervised denoising of images. A noisy input image is decomposed into a set of image patches that are encoded by a graph whose nodes are the patches, and their relative distances form the graph edges. The graph is embedded using the Diffusion Framework, and the resulting Laplacian matrix is used as a denoising operator. Meyer *et al.* proposed to improve the denoising by computing a second embedding using the set of *denoised* patches. The premise is that the intrinsic manifold of the image is encoded by the graph of patches, or equivalently, the eigenfunctions of the corresponding Laplacian matrix. Thus, by computing the second patch graph, a better intrinsic representation of the image is derived, resulting in improved image denoising.

A summary of the different SNL schemes is given in Table I.

III. Sensors Network Localization Using Spectral Regression

In this section we recall the Diffusion framework and its application to sensor localization via spectral regression (SR), as introduced by Keller *et al.* [7]. Let $S = \{\mathbf{x}_i\}_1^N$ be a set of N

sensor nodes, such that $\mathbf{x}_i \in \mathbb{R}^d$ are the vertices of an undirected graph $G = G(V, E)$ and the inter-sensor distances $d_{ij} = \|\mathbf{x}_i - \mathbf{x}_j\|$ are its edges. In order to represent the network by the Diffusion framework, the graph edges are quantified using the RBF kernel

$$w_{ij} = exp\left(-\|\mathbf{x}_i - \mathbf{x}_j\|^2/\sigma^2\right) = exp\left(-d_{ij}^2/\sigma^2\right) \quad (6)$$

where σ is a scale parameter representing the kernel bandwidth. In the SNL problem we set $\sigma \approx R_0/3$, and the affinity $w_{ij} \approx 0\ \forall d_{ij} > R_0$ corresponding to the physical constraints of the SNL problem.

The core of the Diffusion framework is to induce a random walk on the data set S by row-normalizing $\mathbf{W}$ to a Markov matrix $\mathbf{M} = \mathbf{D}^{-1}\mathbf{W}$ where $\mathbf{D}$ is a diagonal matrix such that $d_{ii} = \sum_j w_{ij}$. The eigendecomposition of $\mathbf{M}$ with respect to the Markovian time variable t yields

$$\mathbf{M}^t(\mathbf{x}_i, \mathbf{x}_j) = \sum_l \lambda_l^t \psi_l(\mathbf{x}_i)\phi_l(\mathbf{x}_j) \quad (7)$$

where $\{\lambda_l\}_1^n$ are the eigenvalues of $\mathbf{M}$ and $\{\psi_l\}_1^n$ and $\{\phi_l\}_1^n$ are its corresponding biorthogonal left and right eigenvectors. As the intrinsic dimension of the localization problem is low, the spectrum of $\mathbf{M}$ decays rapidly and it is well approximated by its $l \sim 10$ leading eigenvectors. The Diffusion distance [23] is given by the L_2 norm of difference in probability distributions, and is given in terms of the eigendecomposition of $\mathbf{M}$

$$D_t(\mathbf{x}_i, \mathbf{x}_j)^2 = \sum_{l \geq 1} \lambda_l^{2t} \left(\psi_l(\mathbf{x}_i) - \psi_l(\mathbf{x}_j)\right)^2 \quad (8)$$

This implies that the Diffusion coordinates are given in terms of the eigenvectors and eigenvalues of $\mathbf{M}$, and each sensor (graph node) is mapped to an l-dimensional Diffusion embedding space

$$\Psi : \mathbf{x}_i \mapsto (\lambda_1\psi_1(i), \lambda_2\psi_2(i), \ldots, \lambda_l\psi_l(i))^T \quad (9)$$

such that

$$D_t(\mathbf{x}_i, \mathbf{x}_j)^2 = \|\Psi_t(\mathbf{x}_i) - \Psi_t(\mathbf{x}_j)\|^2. \quad (10)$$

As the SNL problem refers to samples on a non-rectangular and nonuniform domain, the eigenfunctions of the Graph Laplacian, being a generalization of the Fourier transform, serve as basis functions to the samples in that domain [24]. Furthermore, Singer [25] showed that the eigenvectors of the Graph Laplacian reveal the independent components of the source signals, that in the SNL case relate to the x and y coordinates.

The data adaptive bases are given by the embedding eigenvectors $\{\psi_l\}_1^L$, and can be extended to Diffusion Frames by computing a set of M Diffusion bases

$$\Psi_M = \{\Psi_{\sigma_m}\}_1^M = \{\Psi_{\sigma_1}, \ldots, \Psi_{\sigma_m}, \ldots, \Psi_{\sigma_M}\} \quad (11)$$

where $\Psi_\sigma = \{\psi_l^\sigma\}_1^L$ is the diffusion basis derived using a particular bandwidth σ. These bases are defined over the entire network domain, and the x and y coordinates are given by

$$\mathbf{x} = \sum_{l=1}^L a_l\psi_l, \quad \mathbf{y} = \sum_{l=1}^L b_l\psi_l \quad (12)$$

The vectors of coefficients $\mathbf{a}$ and $\mathbf{b}$ are estimated by minimizing the least square fit over the K anchor points. When a Diffusion frame is used with a small number of anchor points, the resulting least squares problem might be underdetermined. For that, L_1 regularization was applied,

$$\mathbf{a}^* = \arg\min_{\mathbf{a}} \left\| \mathbf{x} - \sum_{l=1}^L a_l\psi_l \right\|_2^2 + \lambda^2\|\mathbf{a}\|_1,\ \lambda \in \mathbb{R} \quad (13)$$

allowing to recover the optimal subset of basis functions, while minimizing the regression error. The coefficients $\mathbf{b}$ were computed mutatis mutandis.

IV. Dual Embedding Spectral Regression

The proposed Dual Embedding Spectral Regression (DESR) scheme is an anchor based approach to SNL. The core of our DESR approach is the computation of an adaptive base by computing the dual embedding of the network distances discussed in Section IV-A. This extends the single layer embedding scheme [7], and provides improved localization results. As in prior works [20], [7] the embedding based scheme is used to provide an initial estimate of the localization, that is then refined by applying gradient based optimization. The scheme is summarized in Section IV-D, while Sections IV-A and IV-B introduce the Dual Embedding and Augmented Dual Embedding, respectively, that are the core contributions of this work. A preprocessing step for detecting outlier distance measurements, based on inducing the triangle inequality, is proposed in Section IV-C.

A. Dual Embedding Bases

In order to facilitate the derivation of the Dual Embedding Spectral Regression (DESR) approach, we start by motivating our approach by considering the *US cities* map [7], [20] depicted in Fig. 4(a), whose three leading Diffusion embedding vectors computed as in Section III, are shown in Fig. 3. It follows that these embedding vectors are adapted to the planar domain, but as noticed by Weinberger *et al.* [20], the planar manifold is manifested by a plane embedded in a higher dimensional manifold.

Thus, the gist of the proposed DESR approach is that the adaptive Diffusion basis can be improved by recovering a flat (two-dimensional) parametrization $\Psi^I = \{\psi^I\}_1^L$ by applying an additional embedding into a two-dimensional domain. For that we apply Isomap embedding [26] that explicitly aims to flatten metric datasets by applying multi-dimensional scaling (MDS) to the geodesic distances. This is exemplified by comparing the resulting localization of the *US cities* map in Figs. 4(c)–4(d), to the DESR's two leading embeddings in Figs. 4(g)–4(h). It follows that the resulting DESR localization in Figs. 4(g)–4(h) is better adapted to the geometry of the domain. The domain in Figs. 4(c)–4(d) is moon-like, typical of one-dimensional manifolds embedded in a two-dimensional space.

From a rigorous perspective, the Isomap embedding consists of computing the geodesic distances in the Diffusion embedding domain given by $\Psi = \{\psi_l\}_1^L$. In contrast to the Spectral Regression (SR) approach [7], the Diffusion coordinates Ψ are defined over the entire domain, and the corresponding Diffusion

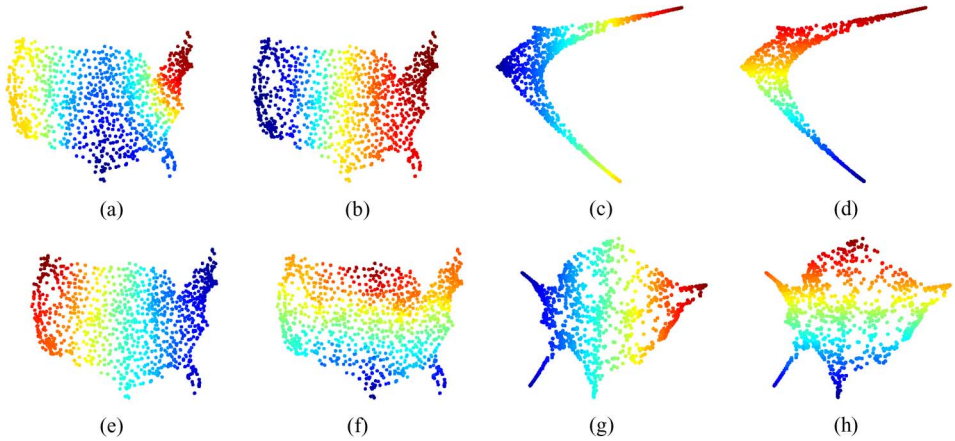

Fig. 4. The Dual Embedding Spectral Regression (DESR). (a) and (b) depict the overlayed values of the leading eigenfunctions (parametrization) of the Diffusion embedding, while (e) and (f) show the corresponding DESR parametrization. The SR-based network localization and corresponding DESR parametrization are shown in Figs. (c)–(d) and (g)–(h), respectively.

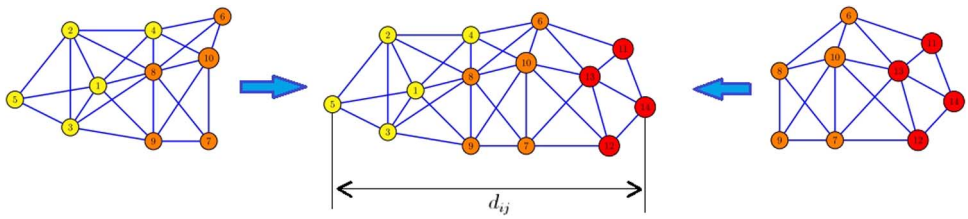

Fig. 5. Computational augmentation of network distances. The two network patches are localized allowing to estimate the distance $d_{5,14}$.

domain geodesic distance matrix $\mathbf{D}_g \in \mathbb{R}_+^{N\times N}$ is dense. This allows the Isomap embedding to utilize N^2 Diffusion distances, rather than the (sparse) $K \cdot N$ ($K \ll N$, $K \approx O(10^{-2}) \cdot N$) distances used by the SR approach.

In that, the proposed approach differs from prior works, such as Meyer *et al.* [22] who applied a dual embedding by reiterating the Diffusion Embedding, where the underlying dataset (image patches in [22]) was reconstructed in the ambient space, and the dual (second layer) embedding was applied to it. The proposed approach operates fully in the embedding domain, as although the sensor network can be reconstructed based on the first layer of embedding (as in the SR approach), we found it provided inferior results.

Thus, given the SR embedding of the sensor network $\Psi = \{\psi_l\}_1^L$, we compute the geodesic distance matrix $\mathbf{D}_g$ and compute its Isomap embeddings $\Psi^I = \{\psi^I\}_1^L$ that serve as the DESR adaptive bases. These are substituted in (12) to estimate the regression coefficients $\mathbf{a}$ and $\mathbf{b}$. In order to utilize the Diffusion Frame [7] the dual embedding is applied to a Diffusion Frame $\Psi_M = \{\Psi_{\sigma_m}\}_1^M$ as in (11), by computing the Isomap embedding $\forall \Psi_{\sigma_m} \in \Psi_M$, yielding the DESR embedding frame

$$\Psi_M^I = \left\{\Psi_{\sigma_1}^I, \ldots, \Psi_{\sigma_M}^I\right\}, \tag{14}$$

where $\Psi_{\sigma_m}^I$ is the dual embedding of Ψ_{σ_m}.

As in [7] the localization is derived by applying L_1 regression to Ψ_M^I to fit the x and y coordinates.

B. Augmented Dual Embedding Bases

Contemporary state-of-the-art SNL schemes start by localizing subsets of sensors into rigid patches, that are globally aligned with respect to rigid transformations [6], [9], [10]. We propose to utilize that school of thought to computationally extend the sensing range R_0. The premise is that the patches are related by multiple noisy node-to-node distances and can thus be used to effectively increase the maximal sensing radius from R_0 to $3R_0$, as depicted in Fig. 5, making the sensor network denser and more rigid.

For that, we localize a set of patches $S_m = \{\mathbf{z}_i\}_1^P$, $P \ll N$ using the Patchwork scheme [9] and its extension by Cucuringu *et al.* [6]. Let $\mathbf{z}_i$ and $\mathbf{z}_j, i \neq j$ be two such patches that are denoted as neighbors if they share common nodes. Neighboring patches are aligned by computing their relative rigid transformation using Least Squares (LS). This allows to estimate a common system of coordinate and compute a dense distance matrix between all of the nodes in $\mathbf{z}_i$ and $\mathbf{z}_j$, that we denote as *computational distances* $D_c = \{d_{ij}^c\}$. This provides additional distance measurements that can be added to the sparse input distance matrix $D = \{d_{ij}\}$ and improve the localization. Indeed, for low noise levels, using the superset of distances

$$D^* = \{D_c, D\} \tag{15}$$

improves the localization.

However, as the noise increases, the Patchwork localization scheme [9] might fail, resulting in inferior localization accuracy. The validity of the additional distances $\{d_{ij}^c\}$ is verified by applying the triangle inequality, and typically a single edge is added such $d_{ij}^c = O(3R_0)$. A motivating example is given in Fig. 6, where we show the improved graph rigidity and resulting localization.

This approach differs from previous works by Zhang *et al.* [10] and Cucuringu *et al.* [6] that recovered the global

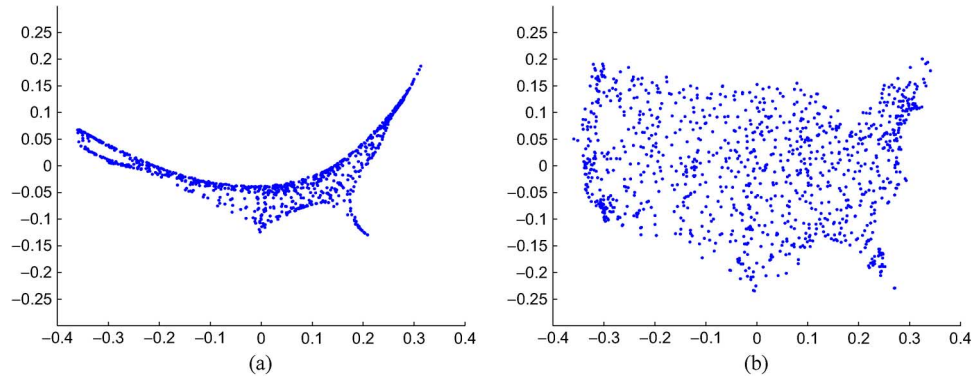

Fig. 6. DESR and ADESR localization of the *USA cities* map using $R_0 = 0.032$, shown in (a) and (b), respectively. The ADESR utilizes additional augmented computational distances.

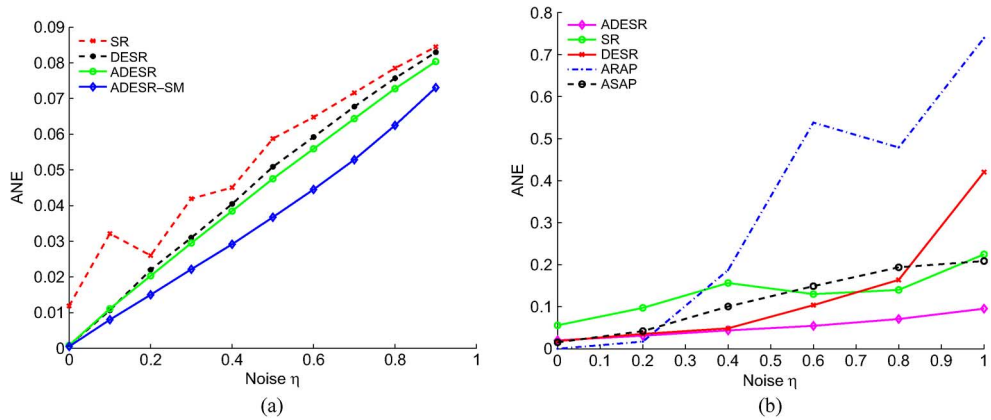

Fig. 7. Localization of the *US cities* network. (a) Localization using $R_0 = 0.1$ comparing different ADESR formulations. (b) Comparing the ARAP, ASAP, DESR and ADESR schemes using $R_0 = 0.032$, where each node is connected to all of the neighboring nodes within R_0. On average $Q \sim 20$.

localization based on the patch alignment parameters. Our approach adds a few 'long' $(O(3R_0))$ geometrically verified distances measurements. Thus, the augmented set of distances D^* is used to form an additional diffusion basis Ψ_P using the procedure discussed in Section III, and its dual embedding $\Psi_{P,I}$ is computed by applying Isomap. The resulting adaptive bases are appended to yield the Augmented DESR (ADESR) diffusion frame

$$\widehat{\Psi} = \{\Psi_\sigma, \Psi_I, \Psi_P, \Psi_{P,I}\}. \tag{16}$$

The localization is recovered by applying the SR approach as in Section III.

C. Preprocessing by Inducing the Triangle Inequality

The SR and DESR approaches are essentially signal processing formulation of the SNL problem, but overlook its geometric interpretation. Namely, the positions of the network's nodes $S = \{\mathbf{x}_i\}_1^N$ must adhere to the Triangle Inequality Theorem. But, as the levels of noise rise, some network triangles might defy the triangle inequality, and can be used to identify outlier distance measurements, denoted as *outlier edges*, as the distance measurements constitute the edges of the sensor network.

We propose to utilize this property as a preprocessing step to the SNL problem, where in order to detect *outlier edges* corrupted by high noise levels, (rather than an outlier triangle), we estimate the probability of an edge to be an outlier, by its probability to be a side of an outlier triangle.

For each network edge e_{ij}, let $T_{ij} = \{T_{ijk}\}$ be the set of triangles such that $e_{ij} \in T_{ijk}$, implying that e_{ij} is a side of T_{ijk}. The triangle inequality is given by upper and lower bounds

$$\begin{aligned} \overline{ij} &> \overline{ik} + \overline{jk} \\ \overline{ij} &< \overline{ik} - \overline{jk} \end{aligned} \tag{17}$$

Let $\{a_{ijk}\}$ be the set of triangle validity indicators, such that

$$a_{ijk} = \begin{cases} 1 & \overline{ij} > \overline{ik} + \overline{jk} \\ -1 & \overline{ij} < \overline{ik} - \overline{jk} \\ 0 & o.w. \end{cases}. \tag{18}$$

The following edge validity measure

$$R_{ij} = \frac{1}{|\{T_{ijk}\}|} \sum_k a_{ijk}, \tag{19}$$

quantifies the probability of an edge to be erroneous. Thus, we propose the a preprocessing step for the input distance measurements $D = \{d_{ij}\}$

$$d'_{ij} = \begin{cases} (1-\alpha)d_{ij}, & R_{ij} > T \\ (1+\beta)d_{ij}, & R_{ij} < -T \\ d_{ij}, & o.w. \end{cases}, \tag{20}$$

where T is a predefined threshold, and α and β are the predefined inflation and deflation coefficients, respectively.

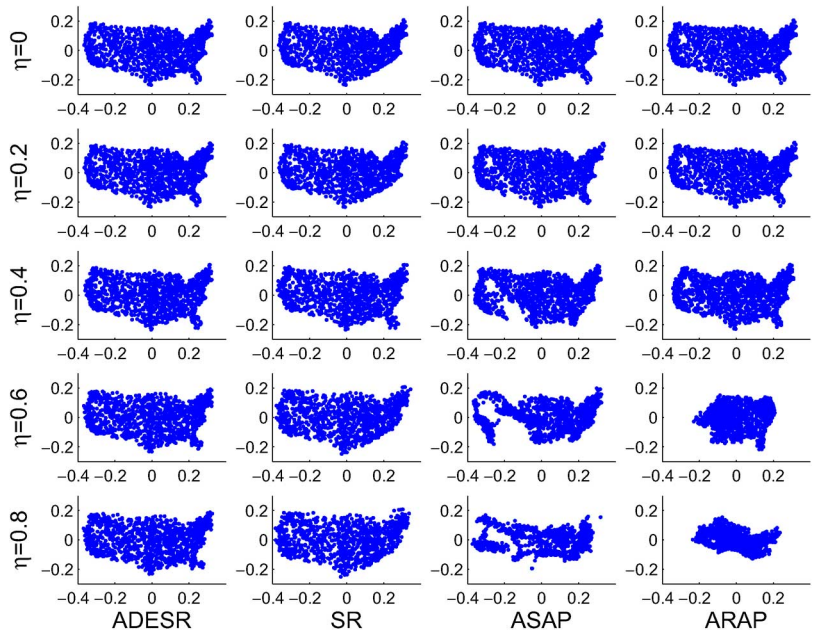

Fig. 8. Localization of the *US cities* network for varying noise levels.

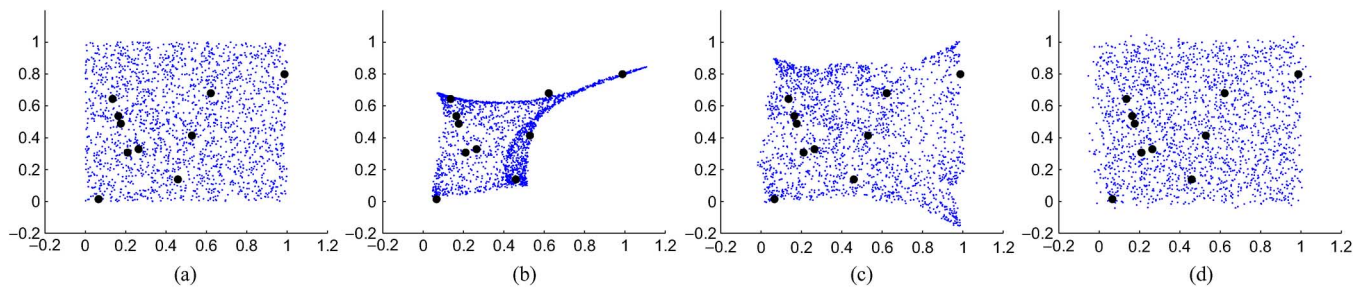

Fig. 9. Localization of the *Random*network using $R_0 = 0.2$, $\eta = 0.9$. (a) Groundtruth network and anchor nodes. (b) SR without SD refinement. (c) ADESR without SD refinement (d) ADESR with SD refinement. (a) Ground truth; (b) SR; (c) ADESR; (d) ADESR with SD.

D. Summary and Implementation Issues

In this section we summarize the overall SNL framework, based on the DESR, ADESR and preprocessing scheme, and detail additional implementation issues.

We start by preprocessing the noisy input distance matrix $D = \{d_{ij}\}$ using the scheme presented in Section IV-C, which allows to disregard erroneous distance measurements. Denote the preprocessed distance matrix D_p. The ADESR scheme introduced in Section IV-B is then applied, by augmenting the number of distance measurements, and computing their dual embedding. This results in the Diffusion frame $\widehat{\Psi}$ (16) consisting of both Diffusion adaptive bases (as in [7]), and their Dual Embedding. By applying L_1 regression as in (12) to the coordinates of the anchor points and $\widehat{\Psi}$, the localization is extended to the entire network. Denote the L_1 regression localization results $S_{L_1} = \{\mathbf{x}_i^{L_1}\}_1^N$.

This provides an initial estimate for localization refinement by applying gradient descent to minimize (3), using the preprocessed distance matrix D_p. Denote the resulting localization $S_{SD} = \{\mathbf{x}_i^{SD}\}_1^N$. In order to account for global transformation, we align S_{SD} to the given K anchor points by estimating a global affine transformation using LS, and apply the SMACOF stress majorization scheme [8] that further improves the localization accuracy.

The distributed implementation of SNL schemes is of particular importance [27]. Hence, we provide an overview of a distributed implementation of the proposed scheme. The preprocessing by inducing the triangle inequality (Section IV-C), the augmentation of the distance measurements (Section IV-B), and the forming of the local sensor patches using the Patchwork scheme [9] and its extension by Cucuringu *et al.* [6], are inherently distributable as they are based on local operations in the spatial vicinity of each sensor. The global computational steps such as the Diffusion embedding and ISOMAP seem to be the more challenging. A decentralized approach for computing the top eigenvectors of a symmetric weighted adjacency matrix using a decentralized implementation of Orthogonal Iteration was proposed by Kempe *et al.* [28], while Magdalinos *et al.* [29] suggested the D-Isomap approach for approximated ISOMAP in large scale P2P networks. A distributed SNL gradient descent and SMACOF schemes were suggested by Zinkevich *et al.* [30] and Jong *et al.* [31], respectively.

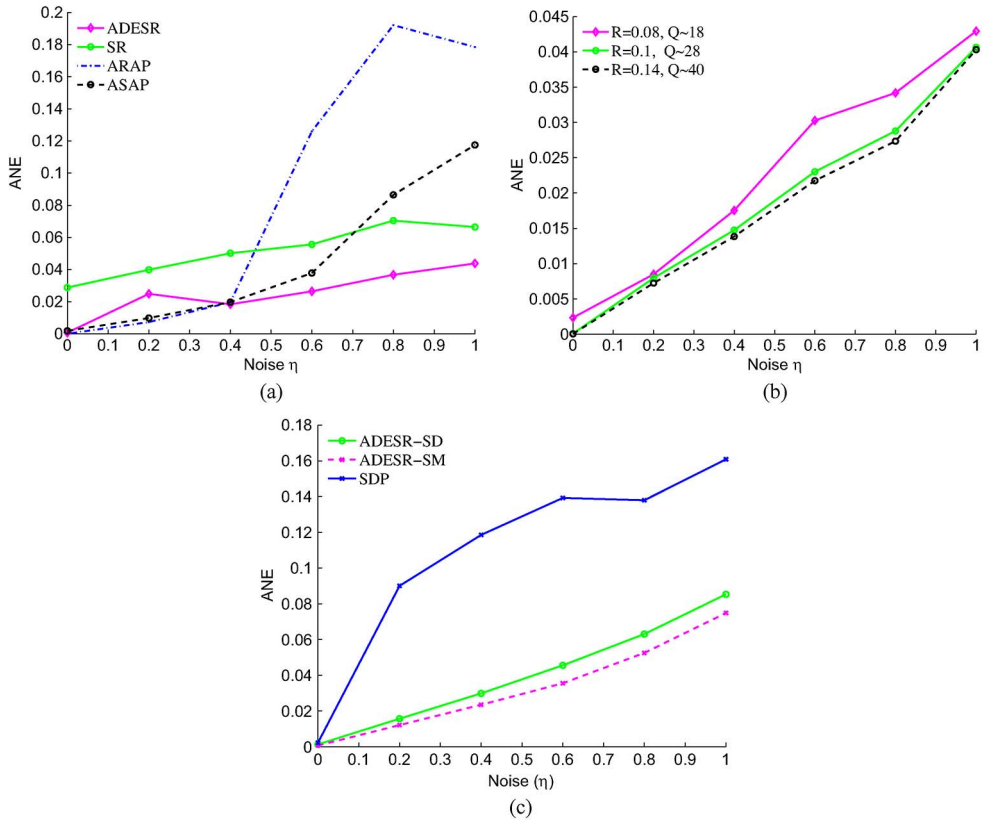

Fig. 10. Localization of the *Random*network depicted in Fig. 9. (a) Localization by ARAP, ASAP, SR and ADESR using $R_0 = 0.08$. (b) DESR with different values of R and their corresponding Q values. (c) Localization of a 272 node random graph using $R_0 = 0.3$, comparing the SR, ADESR with SD refinement and ADESR with SD+SMACOF refinement.

V. Experimental Results

In order to experimentally evaluate the applicability of the proposed schemes we performed exhaustive simulations using synthetic networks, and compared their performance with contemporary state-of-the-art methods. The input to all simulations consisted of a sparse distance matrix $\mathbf{D} = \{d_{ij}\}$, where each node is connected to Q nodes at most, randomly chosen within a sensing radius of R_0. Noise was added to $\mathbf{D}$ according to (1), and K nodes were randomly chosen as anchor points. In all simulations we used $L = 10$ dimensional Diffusion and Isomap embeddings.

The localization accuracy was measured by the Average Normalized Error (ANE) [6], [20]

$$ANE = \frac{\left(\sum_{i,j} \|\mathbf{x}_i - \mathbf{x}_j\|^2\right)^{0.5}}{\left(\sum_i \|\mathbf{x}_i - p_0\|^2\right)^{0.5}} \tag{21}$$

where $p_0 = \frac{1}{N}\sum_n \mathbf{x}_i$.

We compared the proposed scheme against the state-of-the-art ASAP[1] [6], ARAP[2] [10], SR[3] [7] and SDP-SNL[4] [1] schemes, whose code was made available by their authors. The ASAP and ARAP schemes are anchor-free algorithms, but the ASAP can utilize anchor positions to improve localization accuracy. Table II summarizes the notations used for different formulations of the proposed schemes.

The *USA cities* network (Fig. 2(a)) contains 1097 sensors, and was constructed by linking nodes within a radius of $R_0 = 0.1$ and $K = 30$ anchors points. the results of the proposed localization pipeline as well as the SR approach is depicted in Fig. 7(a). We used 120 noise realizations and arbitrary anchors locations for each noise level. As baseline we used the SR approach, and it follows that the DESR and ADESR improve upon the SR, while ADESR-SM provides an additional accuracy gain.

We compared the localization accuracy of the proposed scheme and ASAP and ARAP schemes in Fig. 7(b). These schemes are based on a network model where a node is connected to *all* of its neighbors within the sensing radius R_0. For that we set $R_0 = 0.032$, where on average $Q \approx 20$, and $K = 30$. It follows that the ADESR outperforms all other schemes as the noise level increases.

A qualitative comparison of the *USA cities* network localization is shown in Fig. 8. For low noise levels, all schemes performed similarly. But, as the noise level increases ($\eta > 0.4$), the ASAP and ARAP fail. We attribute that to the failure of their patch localization step that might be susceptible to noise. For $\eta = 0.8$ a foldover is evident in the 'Florida' peninsula of the SR, while the ADESR scheme is able to accurately localize the entire domain.

The ADESR is further qualitatively studied in Fig. 9, where we are given a square consisting of 2000 random nodes, whose

[1]Code available courtesy of the authors.

[2]Code available at: http://www.math.zju.edu.cn/ligangliu/CAGD/Projects/Localization/

[3]Code available courtesy of the authors.

[4]Code available at: http://www.math.nus.edu.sg/mattohkc/SNLSDP.html

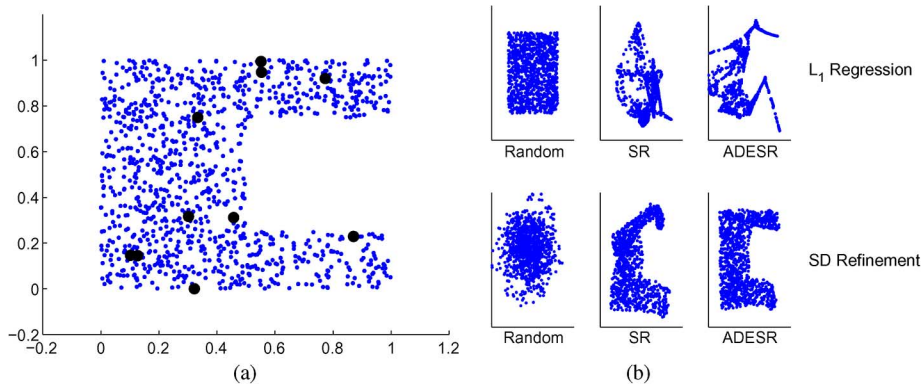

Fig. 11. Localization of the random *C*network. (a) Groundtruth network with overlayed anchor points. (b) top row: localization using varying initial estimates: random, SR and ADESR. (b) bottom row: resulting network localization after applying SD refinement.

distance measurements are corrupted by $\eta = 0.5$ and $K = 10$ anchor points. We compare the spectral regression results of the SR and ADESR schemes without the SD refinement step in Figs. 9(b) and 9(c). The SR shows worse distortion than the ADESR, that provides the most accurate localization depicted in Fig. 9(d).

We repeated the aforementioned simulation with respect to a set of noise realizations and random anchors, where each configuration (noise+anchors) was conducted 120 times and the localization accuracy was averaged. The *Random* network consisted of 1000 nodes, and in Fig. 10(a) we compare the ADESR and SR to the ASAP and ARAP schemes using $R_0 = 0.08$. It follows that for low noise levels ($\eta < 0.4$) the ADESR and ASAP perform similarly, but as the noise level increased the ADESR proved superior. The effect of varying the sensing radius R_0 was studied in Fig. 10(b), where it follows that increasing R_0 improves the localization results. We note that the distance augmentation (Section IV-B) was implemented using the Patchwork scheme [9] and its extension by Cucuringu *et al.* [6]. These approaches assume a disc model where each sensor estimates its distances to *all* of the sensors within a radius R_0. Hence, we were unable to set the number of neighbors Q per sensor explicitly, and report its average.

We compared the SDP-SNL approach to different formulations of the ADESR in Fig. 10(c) using a random graph consisting of 272 nodes, using $R_0 = 0.2$. It follows that the ADESR outperforms the SDP-SNL as the noise level increases. In particular, these results adhere with those reported by Keller *et al.* [7] for other SDP-based SNL schemes [2].

The localization of a nonconvex domain was studied in Fig. 11 where we compare the SR and ADESR to the results of using a random initiation. The network consists of 1100 nodes that were randomly drawn over the domain, $K = 10$ anchors, and we used a sensing radius of $R_0 = 0.1$. Although the outcome of the spectral regression step of the SR and ADESR, shown in the upper row of Fig. 11(b), seems similar, the resulting localization (shown in the bottom row) exemplifies the superiority of the proposed ADESR scheme. The localization based on a random initialization failed due to the nonconvexity of (3). The convergence of the gradient-based refinement is further studied in Section V-C.

Similar qualitative results are reported for the *semi-circle* network shown in Fig. 12. The network consists of 1006 nodes with

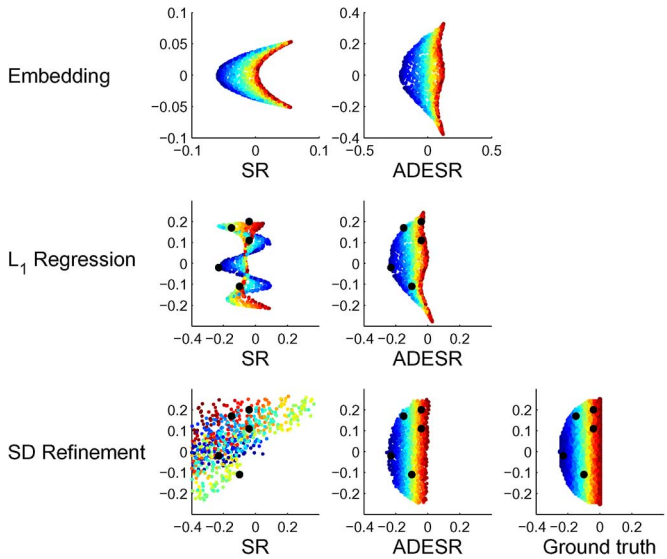

Fig. 12. Qualitative localization results of the *semi-circle* network consisting of 1006 nodes and $K = 5$ anchor points. We used $\eta = 0.5$, $R_0 = 0.1$,. The top row shows the plot of the two leading eigenvectors, while the middle row depicts the localization after the L_1 regression step. The final localization after SD refinement is shown on the bottom row.

TABLE II
NOTATIONS

	ISOMAP	Augmented	SMACOF
SR	-	-	-
DESR	+	-	-
ADESR	+	+	-
ADESR-SM	+	+	+

$\eta = 0.5$ noise, having $K = 5$ anchor points. The sensitivity of the spectral regression and gradient descent based refinement is evident, as the ADESR scheme, in the third column, is the only one able to provide accurate localization.

A. Localization of One-Dimensional Manifolds

The *PACM* network [6] is challenging to localize due to its multiscale structure. While it is globally a two-dimensional network, each of its subnetworks (letters) is essentially a one-dimensional manifold. Fig. 13(a) studies the localization errors

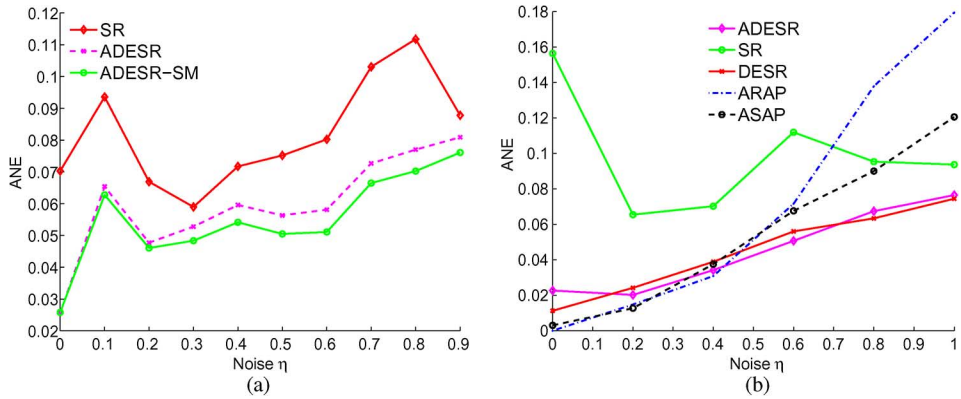

Fig. 13. Quantitative localization results of the *PACM*network. (a) Comparison of the SR, DESR and DESR-SM schemes using $R_0 = 3$. (b) Comparing the ARAP,ASAP, DESR, SR and ADESR using $R_0 = 1.4$. Qualitative results for this network are shown in Fig. 14.

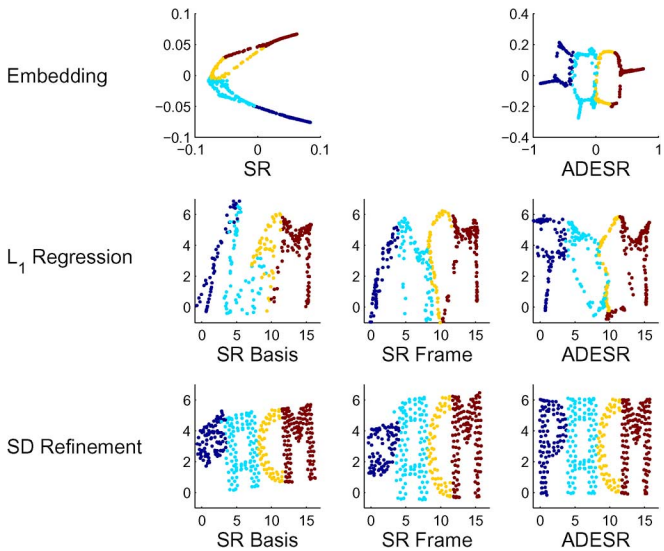

Fig. 14. Qualitative localization results of the *PACM*network, comparing the SR using a single Diffusion basis, SR using a Diffusion Frame and the ADESR. The localization was conducted using $\eta = 0.5$, $R_0 = 2$,. The top row shows the two leading embeddings, while the second row depicts the L_1 regression results. The final localization, after the refinement step, is shown in the last row. Quantitative results for this network are shown in Fig. 13.

with $R_0 = 3$. The ADESR is shown to significantly outperform the SR scheme, where the ADESR-SM shows additional accuracy gain for higher noise values. A comparison against the ASAP and ARAP schemes is shown in Fig. 13(b), where both the DESR and ADESR proved superior.

Fig. 14 depicts the localization pipeline of the *PACM* network with a noise level of $\eta = 0.5$. The ADESR embeddings seem more adapted to domain especially with respect to the leftmost letter ('P'), leading to the superior localization results in the third row.

An additional example of a network whose local structure is essentially one-dimensional is given by the *Spiral* network that is studied in Fig. 15. The ADESR scheme fails to localize the network for $R_0 = 0.4$ as depicted in Fig. 15(a), where the Isomap embedding captures the local one-dimensional manifold of the network and overlooks the global two dimensional network structure. As we increase the sensing radius to $R_0 = 2$, as depicted in Fig. 15(b), the ADESR's Isomap embedding improves, and allows to localize the network.

B. Localization Foldovers Analysis

We study the role of foldovers in the SNL problem in Fig. 16. Foldovers commonly occur in nonrigid regions of the localized network due to lack of a sufficient number of anchors and local network topology. For instance, consider the foldover in the SR reconstruction of the Florida peninsula depicted in Fig. 8. In particular, localization foldovers entail significant localization errors. Fig. 16(a) studies the probability of foldovers occurring with respect to the number of anchor points. The simulations were conducted using the *US Cities* network while varying the number of anchor points K, and adding a noise of $\eta = 0.5$. Each simulation was repeated 300 times and the foldovers statistics were averaged. As K increases the foldovers probability drops, and it is evident that the proposed ADESR scheme significantly reduces the probability of foldovers. In particular, no foldovers occur when applying the ADESR for $K > 10$.

We studied the sensitivity of the foldover probability to varying noise levels in Fig. 16(b), where each simulation was ran 300 times and $K = 30$ was used. We compare the SR, ADESR to ADESR-Pre, which is a variant of ADESR where the input distances were preprocessed by applying the triangle inequality (as in Section IV-C). The ADESR is shown to significantly reduce the number of foldovers, compared to the SR scheme for all noise levels, while the ADESR-Pre improves the robustness further by eliminating all foldovers. In all of our experiments we used the predefined deflation and inflation coefficients $\alpha = 0.1$ and $\beta = 0.2$ as in Section IV-C.

C. Convergence of the Gradient-Based Refinement

The last step of the localization pipeline in embedding-based schemes, such as the MVU, SR and the proposed ADESR, is gradient descent based refinement. Hence, the gist of such schemes is to provides a coarse estimate of the localization that initiates the gradient-based optimization. This was qualitatively exemplified in the previous figures (Figs. 12, 8, 9). In Fig. 17 we study the convergence of the gradient descent step with respect to ADESR-based and groundtruth-based initial estimates. For that we used the C network shown in Fig. 11, that consists of

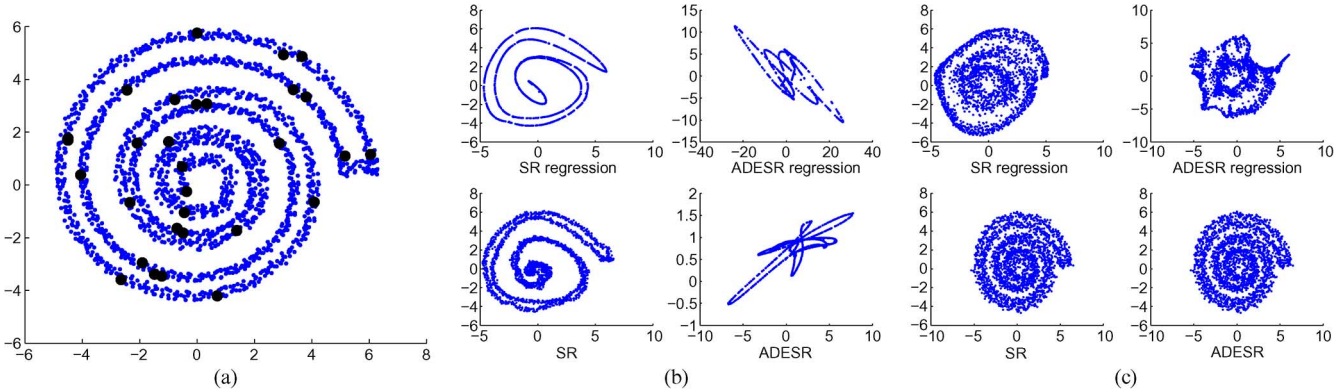

Fig. 15. The localization of the *Spiral* network using varying sensing ranges, and a $\eta = 0.5$ noise level. (a) Groundtruth *Spiral* network and anchor points. The top row of (b) and (c) shows the L_1 regression results, while the bottom row depicts the final localization after the SD refinement step. (a) Spiral network and anchors; (b) $R_0 = 0.4$; (c) $R_0 = 2$.

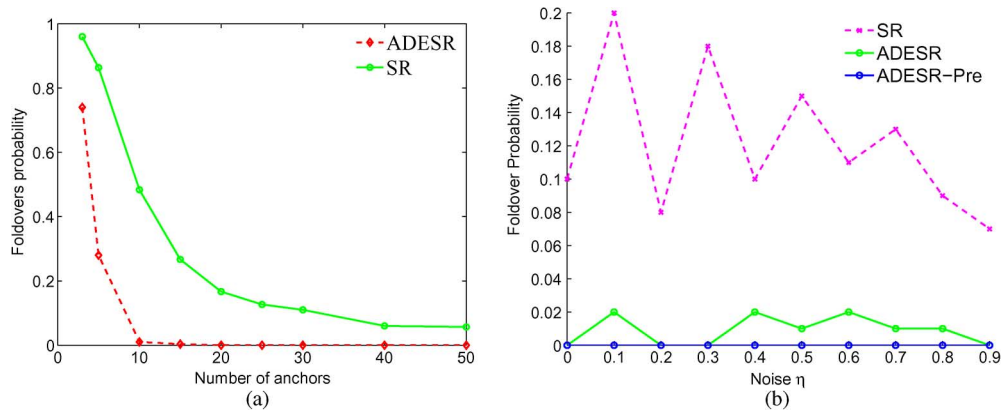

Fig. 16. Analysis of the localization foldovers using *US Cities* network with a noise level of $\eta = 0.5$. (a) The probability of foldovers vs. the number of anchor nodes. (b) The probability of foldovers with respect to varying noise levels using $K = 30$ anchor nodes. The ADESR-Pre scheme applies preprocessing based on the triangle inequality (Section IV-C).

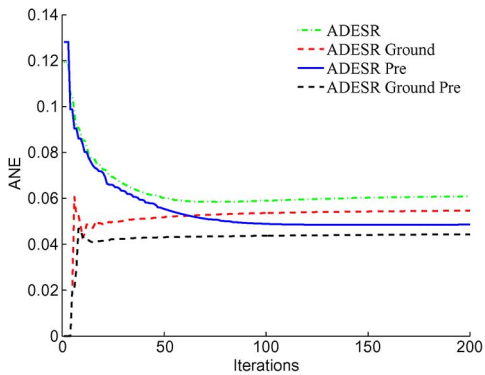

Fig. 17. Convegence analysis of the gradient-based refinement of the ADESR. ADESR and ADESR-Pre are initialized by the L_1 spectral regression, while the 'ADESR Ground' and 'ADESR Ground Pre' are initialized by the groundtruth localization.

1100 nodes, $K = 10$ anchors, a sensing radius of $R_0 = 0.1$. The *compelling* result is that the ADESR-Pre approach that utilizes the triangle inequality based preprocessing (Section IV-C), outperforms the ADESR that utilizes the ground truth as an initial condition. This emphasizes the importance of inducing ambient space-based geometrical constraints (such as the triangle inequality) and paves the way for future work.

TABLE III
TIMING RESULTS

	272 nodes [s]	**1097 nodes [s]**
Dual Embedding	20	190
ARAP-based patch localization	40	220
Augmented distances	20	170
SMACOF-based refinement	60	620
Overall	**140**	**1200**

D. Timing Results

We run the timing simulations on a Core i7 computer, where the proposed scheme was implemented in Matlab and was not optimized for performance. We run random realizations of the 272 nodes random network depicted in Fig. 9 and a 1097 nodes network depicted in Fig. 8. The average running times of the proposed ADESR SNL are reported in Table III, detailing the running time of the different steps of the DESR algorithm. We note that the distance augmentation and patch localization steps can be implemented in a fully parallelized and distributed way on a multicore CPU. Hence, the Dual Embedding that is the core of our approach, requires $\sim$200s on a large network. We conclude that the proposed scheme can be applied to large SNL problems consisting of $\sim o(1000)$ nodes. The localization of larger scale networks would require parallel implementation of the patch localization and distance augmentation schemes.

VI. Conclusions and Future Work

In this work we introduced the DESR approach for sensor networks localization that is based on a dual embedding. It extends the SR approach [7] by applying an additional embedding that better recovers the intrinsic geometry of the sensor network. The DESR is extended by computationally augmenting the network measurements by localizing small network patches. The resulting scheme, denoted as ADESR, is shown to outperform previous state-of-the-art schemes, such as ASAP [6], ARAP [10] and SR [7], in terms of robustness to noise and localization accuracy. We also present a preprocessing scheme based on inducing the triangle inequality that further improves the localization.

We conclude that by aggregating the global network information, and by implicitly inducing low dimensional constraints using the spectral embedding schemes (Diffusion Embedding and Isomap), one can improve the localization, in contrast to recent works ([6], [10]) that agglomerate partial localizations into a global one. Following the improvement we gained by heuristically inducing ambient space geometrical constraints, we aim to derive computational means for inducing such constraints by deriving spectral embeddings that preserve local angles rather than local isometry.

References

[1] P. Biswas, T. C. Lian, T. C. Wang, and Y. Ye, "Semidefinite programming based algorithms for sensor network localization," *ACM Trans. Sen. Netw.*, vol. 2, no. 2, pp. 188–220, 2006.

[2] Z. Wang, S. Zheng, Y. Ye, and S. Boyd, "Further relaxations of the semidefinite programming approach to sensor network localization," *SIAM J. Optimiz.*, vol. 19, no. 2, pp. 655–673, 2008.

[3] P. Biswas, H. Aghajan, and Y. Ye, "Semidefinite programming algorithms for sensor network localization using angle information," in *Proc. 39th Asilomar Conf. Signals, Syst., Comput.*, 2005, pp. 220–224.

[4] K. Q. Weinberger, F. Sha, Q. Zhu, and L. K. Saul, "Graph laplacian regularization for large-scale semidefinite programming," *NIPS*, pp. 1489–1496, 2006.

[5] L. Zhang, L. Liu, C. Gotsman, and S. J. Gortler, "An as-rigid-as-possible approach to sensor network localization," *ACM Trans. Sensor Netw.*, 2010.

[6] M. Cucuringu, Y. Lipman, and A. Singer, "Sensor network localization by eigenvector synchronization over the euclidean group," *ACM Trans. Sensor Netw. (TOSN)*, vol. 8, no. 3, p. 19, 2012.

[7] Y. Keller and Y. Gur, "A diffusion approach to network localization," *IEEE Trans. Signal Process.*, vol. 59, no. 6, pp. 2642–2654, 2011.

[8] I. Borg and P. Groenen, *Modern Multidimensional Scaling: Theory and Applications*. Berlin, Germany: Springer-Verlag, 2005.

[9] Y. Koren, C. Gotsman, and M. Ben-Chen, Patchwork: Efficient Localization for Sensor Networks by Distributed Global Optimization Citeseer, 2005.

[10] L. Zhang, L. Liu, C. Gotsman, and S. J. Gortler, "An as-rigid-as-possible approach to sensor network localization," *ACM Transa. Sensor Netw. (TOSN)*, vol. 6, no. 4, p. 35, 2010.

[11] T. J. V. de Silva and L. J. , "A global geometric framework for nonlinear dimensionality reduction," *Science*, no. 290, pp. 2319–2323, 2000.

[12] P. Biswas, T.-C. Lian, T.-C. Wang, and Y. Ye, "Semidefinite programming based algorithms for sensor network localization," *ACM Trans. Sensor Netw. (TOSN)*, vol. 2, no. 2, pp. 188–220, 2006.

[13] P. Biswas and Y. Ye, "Semidefinite programming for *ad hoc* wireless sensor network localization," in *Proc. 3rd Int. Symp. Inf. Process. Sensor Netw.*, 2004, pp. 46–54, ACM.

[14] A. M.-C. So and Y. Ye, "Theory of semidefinite programming for sensor network localization," *Math. Program.*, vol. 109, no. 2–3, pp. 367–384, 2007.

[15] Z. Zhu, A.-C. So, and Y. Ye, "Universal rigidity: Towards accurate and efficient localization of wireless networks," in *Proc. IEEE INFOCOM*, March 2010, pp. 1–9.

[16] Q. Shi, C. He, H. Chen, and L. Jiang, "Distributed wireless sensor network localization via sequential greedy optimization algorithm," *IEEE Trans. Signal Process.*, vol. 58, no. 6, pp. 3328–3340, 2010.

[17] S. Srirangarajan, A. Tewfik, and Z.-Q. Luo, "Distributed sensor network localization using socp relaxation," *Wireless Communications, IEEE Trans.*, vol. 7, no. 12, pp. 4886–4895, 2008.

[18] T. Eren, O. Goldenberg, W. Whiteley, Y. R. Yang, A. S. Morse, B. D. Anderson, and P. N. Belhumeur, "Rigidity, computation, and randomization in network localization," in *Proc. 23rd Annu. Joint Conf. IEEE Comput. Commun. Soc. (INFOCOM 2004)*, 2004, vol. 4, pp. 2673–2684, IEEE.

[19] D. Moore, J. Leonard, D. Rus, and S. Teller, "Robust distributed network localization with noisy range measurements," in *Proc. 2nd Int. Conf. Embed. Netw. Sensor Syst.*, 2004, pp. 50–61, ACM.

[20] K. Q. Weinberger, F. Sha, Q. Zhu, and L. K. Saul, "Graph laplacian regularization for large-scale semidefinite programming," *Adv. Neural Inf. Process. Syst.*, pp. 1489–1496, 2006.

[21] A. Singer, "A remark on global positioning from local distances," *Proc. Nat. Acad. Sci.*, vol. 105, no. 28, pp. 9507–9511, 2008.

[22] F. G. Meyer and X. Shen, "Perturbation of the eigenvectors of the graph laplacian: Application to image denoising," *Appl. Comput. Harmonic Anal.*, vol. 36, no. 2, pp. 326–334, 2014.

[23] R. R. Coifman and S. Lafon, "Diffusion maps," *Applied and Computational Harmonic Analysis*, vol. 21, no. 1, pp. 5–30, 2006.

[24] N. Saito, "Data analysis and representation on a general domain using eigenfunctions of laplacian," *Appl. Computat. Harmonic Anal.*, vol. 25, no. 1, pp. 68–97, 2008.

[25] A. Singer, "Spectral independent component analysis," *Appl. Comput. Harmonic Anal.*, vol. 21, no. 1, pp. 135–144, 2006.

[26] J. B. Tenenbaum, V. De Silva, and J. C. Langford, "A global geometric framework for nonlinear dimensionality reduction," *Science*, vol. 290, no. 5500, pp. 2319–2323, 2000.

[27] J. A. Costa, N. Patwari, and A. O. Hero, III, "Distributed weighted-multidimensional scaling for node localization in sensor networks," *ACM Trans. Sen. Netw.*, vol. 2, pp. 39–64, Feb. 2006.

[28] D. Kempe and F. McSherry, "A decentralized algorithm for spectral analysis," *J. Comput. Syst. Sci.*, vol. 74, pp. 70–83, Feb. 2008.

[29] P. Magdalinos, M. Vazirgiannis, and D. Valsamou, "Distributed knowledge discovery with non linear dimensionality reduction," in *Advances in Knowledge Discovery and Data Mining*, M. Zaki, J. Yu, B. Ravindran, and V. Pudi, Eds. : Springer Berlin Heidelberg, 2010, vol. 6119, Lecture Notes in Computer Science, pp. 14–26.

[30] M. A. Zinkevich, A. Smola, M. Weimer, and L. Li, "Parallelized stochastic gradient descent," *Adv. Neural Inf. Process. Syst. 23*, pp. 2595–2603, 2010.

[31] J. Y. Choi, S.-H. Bae, X. Qiu, and G. Fox, "High performance dimension reduction and visualization for large high-dimensional data analysis," in *Proc. 10th IEEE/ACM Int. Conf. Cluster, Cloud, Grid Comput. (CCGrid)*, May 2010, pp. 331–340.

Shai Gepshtein received the B.Sc. and M.Sc. degree in electrical engineering from the Tel-Aviv university, Israel, in 1998 and 2004, respectively. From 1998 to 2012, he works as a R&D Engineer. He is currently studying toward the Ph.D. degree in electrical engineering in the Faculty of Engineering, Bar-Ilan University, Ramat-Gan, Israel.

Yosi Keller received the BSc degree in Electrical Engineering in 1994 from the Technion-Israel Institute of Technology, Haifa. He received the MSc and PhD degrees in electrical engineering from Tel-Aviv University, Tel-Aviv, in 1998 and 2003, respectively. From 2003 to 2006 he was a Gibbs assistant professor with the Department of Mathematics, Yale University. He is an Associate Professor at the Faculty of Engineering in Bar Ilan University, Israel.